Impact of Relaxation on the Performance of GeSe True Random Number Generator Based on Ovonic Threshold Switching

Xue Zhou, Zeyu Hu, Zheng Chai, Weidong Zhang, Sergiu Clima, Robin Degraeve, Jian Fu Zhang, Andrea Fantini, Daniele Garbin, Romain Delhougne, Ludovic Goux, and Gouri Sankar Kar

***Abstract*— Volatile Ovonic threshold switching (OTS) are promising not only as the selector in crossbar resistive switching memory arrays, but also as true random number generators (TRNG) by utilizing its probabilistic switching characteristics. However, investigation on the reliability of OTS-based TRNG is still lacking, which hinders its practical application. Previously, we found that switching probability is dependent on the pulse amplitude and width. In this work, we report that relaxation which happens during the time interval between pulses can also cause switching probability drift. Optimizing the bit-generation waveform and modulating the pulse conditions could provide a practical solution, in addition to the impact of external bias and temperature. This work provides useful guidance for the practical design and operation of OTS-based TRNGs.**

***Index Terms*— OTS, GeSe, random number generation, relaxation, threshold voltage.**

I. Introduction

RANDOM number generators (RNGs) are playing pivotal roles in statistical sampling [1], [2], computer simulation [3], cryptography [4], [5], etc. Conventionally, random bit streams are generated using software-based pseudo-RNGs, and inevitably contain repetition and correlation [6]. In contrast, a true random number generator (TRNG) uses physical phenomena as sources of randomness and cannot be replicated or predicted externally. The existing CMOS-based TRNGs are normally based on white noise [7], random telegraph noise (RTN) [8], [9], time-dependent dielectric breakdown [10], or some other noise sources [11]–[16]. However, in those TRNG implementations, complex signal post-processing systems are required, leading to increasing scaling difficulty.

Earlier works have reported that the Ovonic threshold switching (OTS) chalcogenide materials, a promising material for selector applications in emerging memory arrays [17]–[20], can also work as a randomness source by exploiting its randomly distributed time-to-switch-on/off [21]–[23]. The volatile nature of OTS offers an important advantage, as it avoids the reset operation in TRNGs based on non-volatile memory devices for erasing the previous generated bit, thus simplifying the circuitry, and improving the throughput. Our preliminary exploration of OTS-based TRNG shows satisfying randomness in 10,000 bits [21] and its promising potential in the application of stochastic computing [23]. However, further reliability investigation under variable operation conditions is still needed for the practical TRNG application.

In this work, we further look into the switching probability drift in OTS-based TRNGs using statistical measurements, and attributed it to the relaxation phenomenon in chalcogenide after switching, which leads to threshold voltage (V_{th}) drift. Such relaxation can be accelerated by using external bias or higher temperature, however, optimizing the bit-generation waveform and modulating the pulse conditions is a more practical solution for TRNG circuitry. This work provides useful guidance for the practical design and operation of OTS-TRNGs.

II. Device and Characterization

Amorphous Ge_xSe_{1-x} films were sandwiched between two TiN electrodes to form a TiN/Ge_xSe_{1-x}/TiN structure. The OTS devices were integrated in a 300 nm process flow and device size is defined by the TiN bottom electrode [24]. The Ge_xSe_{1-x} chalcogenide films were deposited and passivated by a low-temperature BEOL process scheme, as shown in Fig. 1a. The device size is 65 nm and the Ge_xSe_{1-x} thickness is 10 nm. The fast I-V characterization was done with a Keysight B1500A semiconductor analyzer with embedded B1530A Waveform Generator/Fast Measurement Unit (WGFMU). Fig. 1b schematizes the random generation

Manuscript received April 11, 2022; revised May 13, 2022; accepted May 30, 2022. Date of publication June 1, 2022; date of current version June 30, 2022. This work was supported in part by the National Natural Science Foundation of China under Grant 62104188; in part by the Major Key Project of Peng Cheng Laboratory (PCL) under Grant PCL2021A12; and in part by the Engineering and Physical Sciences Research Council (EPSRC), U.K., under Grant EP/M006727/1 and Grant EP/S000259/1. The review of this letter was arranged by Editor U. Ganguly. *(Corresponding authors: Zheng Chai; Weidong Zhang.)*

Xue Zhou and Zheng Chai are with the State Key Laboratory for Mechanical Behavior of Materials, the Center for Spintronics and Quantum Systems, and the School of Materials Science and Engineering, Xi'an Jiaotong University, Xi'an 710049, China, also with the Peng Cheng Laboratory, Shenzhen 518055, China, and also with the Pazhou Laboratory (Huangpu), Guangzhou 510555, China (e-mail: zheng.chai@xjtu.edu.cn).

Zeyu Hu, Weidong Zhang, and Jian Fu Zhang are with the School of Engineering, Liverpool John Moores University, Liverpool L3 3AF, U.K. (e-mail: w.zhang@ljmu.ac.uk).

Sergiu Clima, Robin Degraeve, Andrea Fantini, Daniele Garbin, Romain Delhougne, Ludovic Goux, and Gouri Sankar Kar are with imec, 3001 Leuven, Belgium.

Color versions of one or more figures in this letter are available at https://doi.org/10.1109/LED.2022.3179590.

Digital Object Identifier 10.1109/LED.2022.3179590

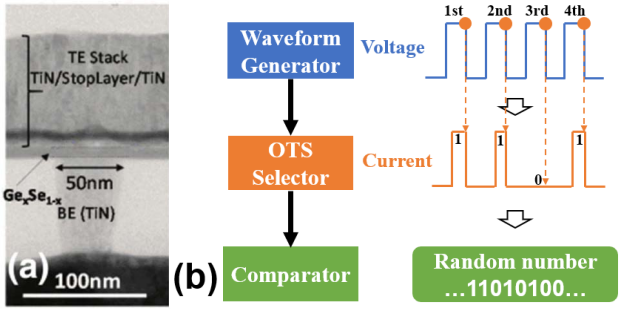

Fig. 1. (a) TEM of a Ge_xSe_{1-x} OTS selector. (b) Schematic of the random generation procedure, including a waveform generator, an OTS selector and a comparator to provide digital "1" and "0". Current is measured at the end of each pulse. Digital bits "1" or "0" are generated by a comparator, depending whether OTS has been switched on or not.

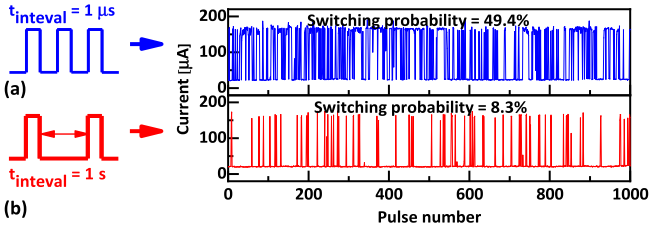

Fig. 2. Demonstration of the current measured in 1000 pulses (V_{pulse} = 2.7 V, t_{pulse} = 1 μs), with interval time of (a) 1 μs and (b) 1 s respectively. The switching probability drops significantly with longer interval time.

procedure in our previous work [21], [23]: A sequence of pulses generated by a waveform generator is applied onto the top electrode of OTS, while the current is measured from the bottom electrode at a certain point of each pulse. Digital bits "1" or "0" are generated by a comparator, depending whether OTS has been switched on at this measurement point.

III. Results and Discussions

Our previous works revealed that the stochastic switching of OTS originates from the Weibull-distribution of time-to-switch-on (t-on) [21], [23], [25]. Particularly, [23] shows that switching probability can be tuned by the pulse amplitude or pulse width. For a practical TRNG, it is also desirable that the TRNG works stably under different pulse intervals, i.e. the switching probability does not drift with different interval time between pulses. Unfortunately, using the previously proposed setup [21], [23], the switching probability drops significantly if the pulse interval increases from 1 μs to 1 s (Fig.2), with a fixed pulse amplitude of 2.7 V and pulse width of 1 μs.

The impact of interval time is further analyzed using a train of triangular pulses with the same amplitude (5 V) and rise/fall time (1 μs) but increasing interval times (Fig. 3a). The benefit of using triangular pulses is to precisely monitor the voltage as well as the time in OTS switching [17], [25]. A higher amplitude of 5.5 V is applied to first-fire a fresh device and 100 triangular pulses with interval of 1 μs are then applied to stabilize the device. Following that, the triangular pulse train in Fig. 3a starts. The 1st V_{th} is around 2.9 V, while the 2nd Vth after an interval of 1 μs becomes much lower (2.5 V). However, the following V_{th}s gradually "recovers" after longer interval time, and could even surpass the 1st V_{th} if the interval reaches 1000 s (Fig. 3b). Such V_{th} recovery is statistically verified using a designed waveform with two

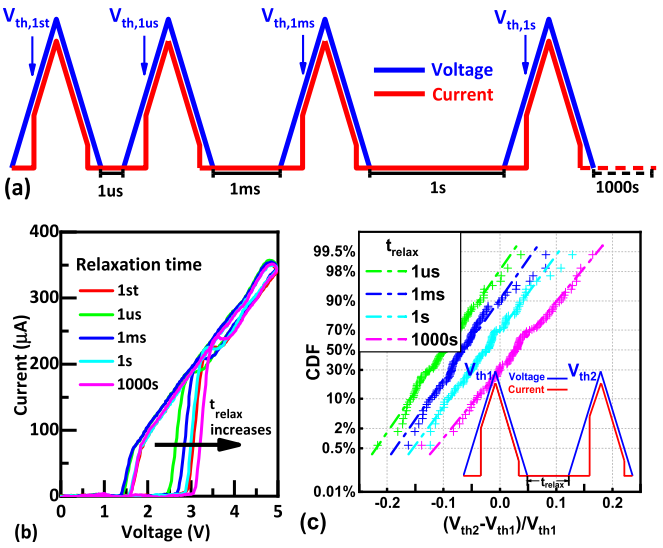

Fig. 3. (a) A train of triangular pulses with increasing interval times to analyse the impact of interval time on V_{th}. (b) V_{th} increases with longer relaxation time. (c) Statistical distribution of V_{th} with different interval time measured using the (inset) sandwiched waveform.

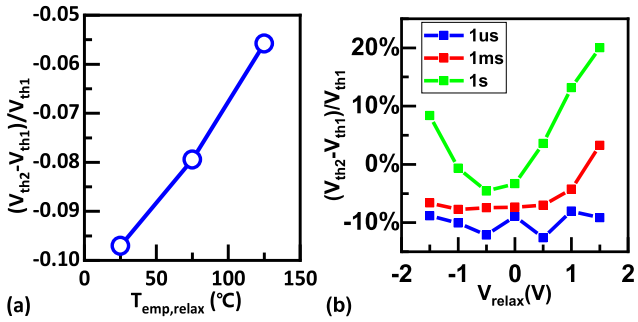

Fig. 4. Relaxation under different temperature and bias conditions, under sandwiched triangular pulses in Fig. 3c. (a) The median $(V_{th2}-V_{th1})/V_{th1}$ at different temperatures with V_{relax} fixed at 0V and relaxation time of 1 μs. (b) The median $(V_{th2}-V_{th1})/V_{th1}$ at different V_{relax} at 25°c with relaxation time of 1 μs, 1 ms and 1s.

triangular pulses sandwiched with an interval period (inset in Fig. 3c). For each interval time, the sandwiched waveform is repeated for 100 times, with a fixed gap period of 10 s in between. Obviously, for each interval time, V_{th} follows normal distribution, which shifts rightward with longer interval times, (Fig. 3c).

Such V_{th} recovery phenomenon could explain the change in switching probability at longer intervals proposed in Fig. 2: (i) the longer interval time between each square pulse leads to a higher V_{th}; (ii) moreover, a failure-to-switch-on by one pulse effectively prolongs the relaxation period and further increases the V_{th}, making it more difficult to switch-on by the next pulse. Therefore, the relaxation issue could be the main reason for the probability drift of OTS-based TRNG when interval time varies.

The V_{th} recovery of OTS is associated with the delocalization of defects [26]. After the switch-off, some defects remain delocalized, leading to a reduced V_{th} in subsequent switching. During relaxation, the remaining delocalized defects gradually return to the localized state, and thus a higher voltage is needed to delocalize those defects, leading to a higher V_{th} [17].

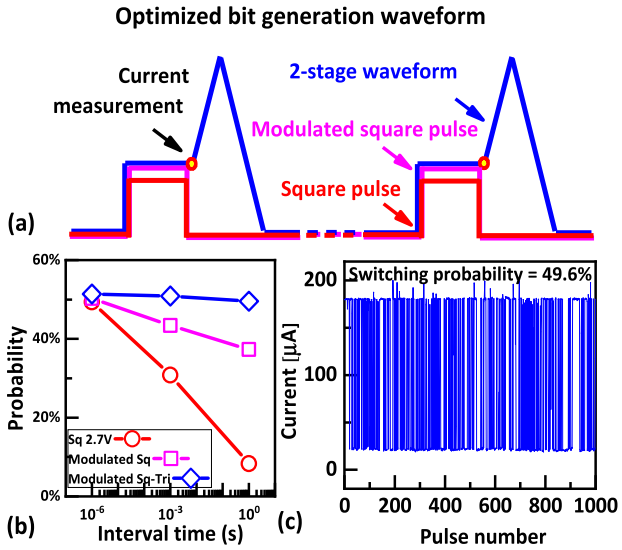

Fig. 5. (a) The optimized 2-stage "square-triangular" waveform to remove the cumulative effect of failure-to-switch-on. Current is measured at the end of the square pulse. (b) Comparison of the switching probability measured with various interval time (○) using square pulse of 2.7 V, (□) modulated square pulse of 2.7 V, 2.8 V and 2.9 V for interval time of 1 us, 1 ms and 1 s, respectively and (◇) 2-stage square-triangular pulse with square pulse amplitude being modulated in the same way as in (□). (c) Random bit stream generated with interval time = 1 s using the 2-stage square-triangular waveform with modulated square pulse amplitude (◇).

Therefore, external conditions that affects the localization process should also change the relaxation rate. The sandwiched waveform used in Fig. 3c (with a fixed pulse interval of 1 μs) is repeated for 100 times under different temperatures ($T_{emp,\ relax}$) (Fig. 4a) or with varying relaxation bias V_{relax} (Fig. 4b). It shows that measuring at higher temperatures or applying a bias voltage during the interval could both accelerate the relaxation.

Although V_{th} recovery can be accelerated at higher temperature and/or with a relaxation bias, those methods are not convenient to implement in practical TRNG circuits, either requiring heating components or increasing power consumption. A practical solution might be obtained from the operational perspective, by optimizing the bit-generation waveform and modulating the pulse conditions: (i) the higher V_{th} caused by the relaxation at longer interval times could be compensated by using a higher square pulse amplitude, inspired by the dependence of V_{th} on the bias condition as we have reported in [23], [25]; and (ii) in order to further remove the cumulative effect of failure-to-switch-on, a 2-stage "square-triangular" waveform, in which the current is measured at the end of the square pulse, is used to ensure that OTS is switched on after generating each bit, no matter "0" or "1", (Fig. 5a), avoiding the need for complex peripheral circuitry to distinguish whether the OTS has been switched on or not during the square stage.

To verify this method, a sequence of 1000 square-triangular waveform pulses with higher square pulse for longer interval time, i.e. modulated square pulse, is applied to this OTS device. The square pulse amplitudes are 2.7 V, 2.8 V and 2.9 V for interval time of 1 μs, 1 ms and 1 s, respectively. The triangular pulse starts from the end of the square pulse, reaches its peak of 5 V, and then falls to 0 V (t_{fall} = 1 μs). Fig. 5b

TABLE I
NIST TEST RESULT

Test	p-value	Proportion	Result
Frequency	0.739918	10/10	Pass
Block Frequency	0.534146	10/10	Pass
Runs	0.739918	10/10	Pass
Longest Run	0.534146	10/10	Pass
FFT	0.350485	10/10	Pass
Cumulative Sums	0.350485*	10/10	Pass
Linear Complexity	0.534146	10/10	Pass
Approximate entropy	0.739918	10/10	Pass
Non- Overlapping Template	0.066882*	10/10	Pass
Overlapping Template	0.122325*	10/10	Pass
Serial	0.066882*	10/10	Pass
Rank	0.350485	1/1	Pass

The sequence is divided into 10 streams, except the Rank test
**Smallest of the multiple p-values*

demonstrates that, by using the modulated square pulses, the probability shift caused by longer interval is reduced significantly and using the 2-stage square-triangular pulse with modulated square pulses could effectively keep the switching probability at around 50%.

The randomness of the bits produced was evaluated by the National Institute of Standards and Technology (NIST) Test Suite, a statistical package to evaluate the randomness of binary sequences. Table I summarized the test result for the 10,000 random bits generated by the TRNG, using the 2-stage square-triangular pulse with modulated square pulse amplitude, as reported in Fig. 5b. The interval time is 1 s. Each test calculates a p-value, and $p>0.001$ and success proportion of 9/10 are considered good performance. Note that some of the tests consist of several individual tests and we report the smallest p-value out of them. The generated random sequences have passed 12 NIST tests, supporting an excellent randomness performance of the proposed TRNG.

It should be noted that applying a higher pulse based on longer interval time setup, or sending a 2-stage waveform, is much simpler than designing a complex peripheral circuitry with counters and registers which increase the layout overhead and also cause major reduction in the throughput of random bit generation, as the data post-processing can be time consuming. Our result shows that although the V_{th} relaxation is an unavoidable nature of chalcogenide materials, its impact could be conveniently controlled using waveform optimization and condition modulation.

IV. CONCLUSION

In this work, we statistically look into the mechanism of switching probability drift in OTS-based TRNG, and have revealed that such switching probability drift can be caused by the relaxation phenomenon in chalcogenide materials after switching-on. Experimental evidence has revealed that relaxation can be accelerated with external bias/temperature, but optimizing the bit-generation waveform and modulating the pulse conditions might be a more practical solution. This work paves the way towards the practical design and operation of OTS-based TRNGs.

REFERENCES

[1] S. Raychaudhuri, "Introduction to Monte Carlo simulation," in *Proc. Winter Simul. Conf.*, Miami, FL, USA, Dec. 2008, pp. 91–100, doi: 10.1109/WSC.2008.4736059.

[2] P. Shukla, A. Shylendra, T. Tulabandhula, and A. R. Trivedi, "MC2RAM: Markov chain Monte Carlo sampling in SRAM for fast Bayesian inference," in *Proc. IEEE Int. Symp. Circuits Syst. (ISCAS)*, Seville, Spain, Oct. 2020, pp. 1–5, doi: 10.1109/ISCAS45731.2020.9180701.

[3] J. E. Gentle, *Random Number Generation and Monte Carlo Methods*. New York, NY, USA: Springer-Verlag, 1998, doi: 10.1007/978-1-4757-2960-3.

[4] C. S. Petrie and J. A. Connelly, "A noise-based IC random number generator for applications in cryptography," *IEEE Trans. Circuits Syst. I, Fundam. Theory Appl.*, vol. 47, no. 5, pp. 615–621, May 2000, doi: 10.1109/81.847868.

[5] S. Kalanadhabhatta, D. Kumar, K. K. Anumandla, S. A. Reddy, and A. Acharyya, "PUF-based secure chaotic random number generator design methodology," *IEEE Trans. Very Large Scale Integr. (VLSI) Syst.*, vol. 28, no. 7, pp. 1740–1744, Jul. 2020, doi: 10.1109/TVLSI.2020.2979269.

[6] F. James and L. Moneta, "Review of high-quality random number generators," *Comput. Softw. Big Sci.*, vol. 4, no. 1, pp. 1–12, Dec. 2020, doi: 10.1007/s41781-019-0034-3.

[7] W. A. G. Rojas, J. J. Mcmorrow, M. L. Geier, Q. Tang, C. H. Kim, T. J. Marks, and M. C. Hersam, "Solution-processed carbon nanotube true random number generator," *Nano Lett.*, vol. 17, no. 8, pp. 4976–4981, Aug. 2017, doi: 10.1021/acs.nanolett.7b02118.

[8] J. Brown, R. Gao, Z. Ji, J. Chen, J. Wu, J. Zhang, B. Zhou, Q. Shi, J. Crowford, and W. Zhang, "A low-power and high-speed true random number generator using generated RTN," in *Proc. IEEE Symp. VLSI Technol.*, Honolulu, HI, USA, Jun. 2018, pp. 95–96, doi: 10.1109/VLSIT.2018.8510671.

[9] Z. Ji, J. Brown, and J. Zhang, "True random number generator (TRNG) for secure communications in the era of IoT," in *Proc. China Semiconductor Technol. Int. Conf. (CSTIC)*, Shanghai, China, Jun. 2020, pp. 1–5, doi: 10.1109/CSTIC49141.2020.9282535.

[10] N. Liu, N. Pinckney, S. Hanson, D. Sylvester, and D. Blaauw, "A true random number generator using time-dependent dielectric breakdown," in *Symp. VLSI Circuits Dig. Tech. Papers*, Kyoto, Japan, Jun. 2011, pp. 216–217.

[11] H. Jiang, D. Belkin, S. E. Savel'ev, S. Lin, Z. Wang, Y. Li, S. Joshi, R. Midya, C. Li, M. Rao, M. Barnell, Q. Wu, J. Yang, and Q. Xia, "A novel true random number generator based on a stochastic diffusive memristor," *Nature Commun.*, vol. 8, p. 882, Oct. 2017, doi: 10.1038/s41467-017-00869-x.

[12] U. Guler, A. E. Pusane, and G. Dundar, "Investigating flicker noise effect on randomness of CMOS ring oscillator based true random number generators," in *Proc. Int. Conf. Inf. Sci., Electron. Electr. Eng.*, Sapporo, Japan, Apr. 2014, pp. 845–849, doi: 10.1109/InfoSEEE.2014.6947786.

[13] V. R. Pamula, X. Sun, S. M. Kim, F. U. Rahman, B. Zhang, and V. S. Sathe, "A 65-nm CMOS 3.2-to-86 Mb/s 2.58 pJ/bit highly digital true-random-number generator with integrated de-correlation and bias correction," *IEEE Solid-State Circuits Lett.*, vol. 1, no. 12, pp. 237–240, Dec. 2018, doi: 10.1109/LSSC.2019.2896777.

[14] N. K. Saligedar, M. Mosazadeh, and A. Khoie, "A true random number generator robust against PVT variation," in *Proc. Iranian Conf. Electr. Eng. (ICEE)*, Mashhad, Iran, May 2018, pp. 120–124, doi: 10.1109/ICEE.2018.8472413.

[15] H. Guo, W. Tang, Y. Liu, and W. Wei, "Truly random number generation based on measurement of phase noise of a laser," *Phys. Rev. E, Stat. Phys. Plasmas Fluids Relat. Interdiscip. Top.*, vol. 81, no. 5, May 2010, Art. no. 051137, doi: 10.1103/PhysRevE.81.051137.

[16] H. Mulaosmanovic, T. Mikolajick, and S. Slesazeck, "Random number generation based on ferroelectric switching," *IEEE Electron Device Lett.*, vol. 39, no. 1, pp. 135–138, Jan. 2018, doi: 10.1109/LED.2017.2771818.

[17] Z. Chai, W. Zhang, R. Degraeve, S. Clima, F. Hatem, J. F. Zhang, P. Freitas, J. Marsland, A. Fantini, D. Garbin, L. Goux, and G. S. Kar, "Evidence of filamentary switching and relaxation mechanisms in Ge_xSe_{1-x} OTS selectors," in *Proc. Symp. VLSI Technol.*, Kyoto, Japan, Jun. 2019, pp. T238–T239, doi: 10.23919/VLSIT.2019.8776566.

[18] Z. Chen, H. Tong, W. Cai, L. Wang, and X. Miao, "Modeling and simulations of the integrated device of phase change memory and ovonic threshold switch selector with a confined structure," *IEEE Trans. Electron Devices*, vol. 68, no. 4, pp. 1616–1621, Apr. 2021, doi: 10.1109/TED.2021.3059436.

[19] S. Lee, J. Lee, S. Kim, D. Lee, D. Lee, and H. Hwang, "Mg-Te OTS selector with low I_{off} (<100 pA), fast switching speed (τd=7 ns), and high thermal stability (400 °C/30 min) for X-point memory applications," in *Proc. Symp. VLSI Technol.*, Kyoto, Japan, 2021, pp. 1–2.

[20] Y. Koo, S. Lee, S. Park, M. Yang, and H. Hwang, "Simple binary ovonic threshold switching material SiTe and its excellent selector performance for high-density memory array application," *IEEE Electron Device Lett.*, vol. 38, no. 5, pp. 568–571, May 2017, doi: 10.1109/LED.2017.2685435.

[21] Z. Chai, P. Freitas, J. Marsland, A. Fantini, D. Garbin, L. Goux, G. S. Kar, W. Shao, W. Zhang, J. Brown, R. Degraeve, F. D. Salim, S. Clima, F. Hatem, and J. F. Zhang, "GeSe-based ovonic threshold switching volatile true random number generator," *IEEE Electron Device Lett.*, vol. 41, no. 2, pp. 228–231, Feb. 2020, doi: 10.1109/LED.2019.2960947.

[22] M. Kwak, S. Lee, W. Choi, C. Lee, S. Kim, and H. Hwang, "OTS-based analog-to-stochastic converter for fully-parallel weight update in cross-point array neural networks," in *Proc. Symp. VLSI Technol.*, Kyoto, Japan, 2021, pp. 1–2.

[23] Z. Chai, P. Freitas, W. D. Zhang, F. Hatem, R. Degraeve, S. Clima, J. F. Zhang, J. Marsland, A. Fantini, D. Garbin, L. Goux, and G. S. Kar, "Stochastic computing based on volatile GeSe ovonic threshold switching selectors," *IEEE Electron Device Lett.*, vol. 41, no. 10, pp. 1496–1499, Oct. 2020, doi: 10.1109/LED.2020.3017095.

[24] B. Govoreanu, G. L. Donadio, K. Opsomer, W. Devulder, V. V. Afanas'ev, T. Witters, S. Clima, N. S. Avasarala, A. Redolfi, S. Kundu, O. Richard, D. Tsvetanova, G. Pourtois, C. Detavemier, L. Goux, and G. S. Kar, "Thermally stable integrated Se-based OTS selectors with >20 MA/cm^2 current drive, >3.10^3 half-bias nonlinearity, tunable threshold voltage and excellent endurance," in *Proc. Symp. VLSI Technol.*, Kyoto, Japan, 2017, pp. T92–T93, doi: 10.23919/VLSIT.2017.7998207.

[25] Z. Chai, W. Zhang, R. Degraeve, S. Clima, F. Hatem, J. F. Zhang, P. Freitas, J. Marsland, A. Fantini, D. Garbin, L. Goux, and G. S. Kar, "Dependence of switching probability on operation conditions in Ge_xSe_{1-x} ovonic threshold switching selectors," *IEEE Electron Device Lett.*, vol. 40, no. 8, pp. 1269–1272, Aug. 2019, doi: 10.1109/LED.2019.2924270.

[26] D. Garbin, W. Devulder, R. Degraeve, G. L. Donadio, S. Clima, K. Opsomer, A. Fantini, D. Cellier, W. G. Kim, M. Pakala, A. Cockburn, C. Detavernier, R. Delhougne, L. Goux, and G. S. Kar, "Composition optimization and device understanding of Si-Ge-As-Te ovonic threshold switch selector with excellent endurance," in *IEDM Tech. Dig.*, San Francisco, CA, USA, Dec. 2019, pp. 35.1.1–35.1.4, doi: 10.1109/IEDM19573.2019.8993547.